Supplement of Atmos. Chem. Phys., 15, 1823–1841, 2015
http://www.atmos-chem-phys.net/15/1823/2015/
doi:10.5194/acp-15-1823-2015-supplement

Atmospheric Chemistry and Physics
Open Access

*Supplement of*

# Mixing state of carbonaceous aerosol in an urban environment: single particle characterization using the soot particle aerosol mass spectrometer (SP-AMS)

**A. K. Y. Lee et al.**

*Correspondence to:* A. K. Y. Lee (klee@chem.utoronto.ca)

## Tables:

Table S1: The refractory black carbon (rBC) column of the fragmentation table in Squirrel.

| m/z | frag_organic | frag_rBC[#] | rBC fragments |
|---|---|---|---|
| 12 | 12,-frag_rBC[12] | 0.61*frag_rBC[36] | $C_1^+$ |
| 24 | | 24,-frag_sulfate[24] | $C_2^+$ |
| 36 | | 36,-frag_air[36] | $C_3^+$ |
| 48 | 0.5*frag_organic[62] | 0.057*frag_rBC[36] | $C_4^+$ |
| 60 | 60,-frag_rBC[60] | 0.047*frag_rBC[36] | $C_5^+$ |

[#] The $C_1/C_3$ ratio of ambient rBC was determined using the $C_1/C_3$ ratio of Regal Black, and the $C_4/C_3$ and $C_5/C_3$ ratios of ambient rBC were determined using the high resolution fitting data of ambient measurements.

Table S2: The simplified fragmentation patterns of each aerosol species for the calculation of chemical compositions for individual single particles from UMR cluster results.

| **Aerosol species** | **The simplified fragmentation patterns** |
|---|---|
| Total | All ions – m/z 14 ($N^+$) – m/z 15 ($NH^+$) – m/z 16 ($NH_2^+$) – m/z 17 ($NH_3^+$) – m/z 18 ($H_2O^+$) – m/z 28 ($N_2^+$) – m/z 32 ($O_2^+$) – m/z 39 ($K^+$) |
| Nitrate | m/z 30 ($NO^+$) + m/z 46 ($NO_2^+$) |
| Sulfate | (m/z 48 - 0.047*m/z 36) ($SO^+$) + m/z 64 ($SO_2^+$) + 0.203*m/z 64 ($HSO_2^+$) + m/z 80 ($SO_3^+$) + 0.926*m/z 80 ($HSO_3^+$) + m/z 98 ($H_2SO_4^+$) |
| rBC | 0.61*m/z 36 ($C^+$) + m/z 24 ($C_2^+$)+ m/z 36 ($C_3^+$) + 0.057*m/z 36 ($C_4^+$) + 0.047*m/z 36 ($C_5^+$) |
| Organics | Total – Nitrate – Sulfate – rBC |

## Figures:

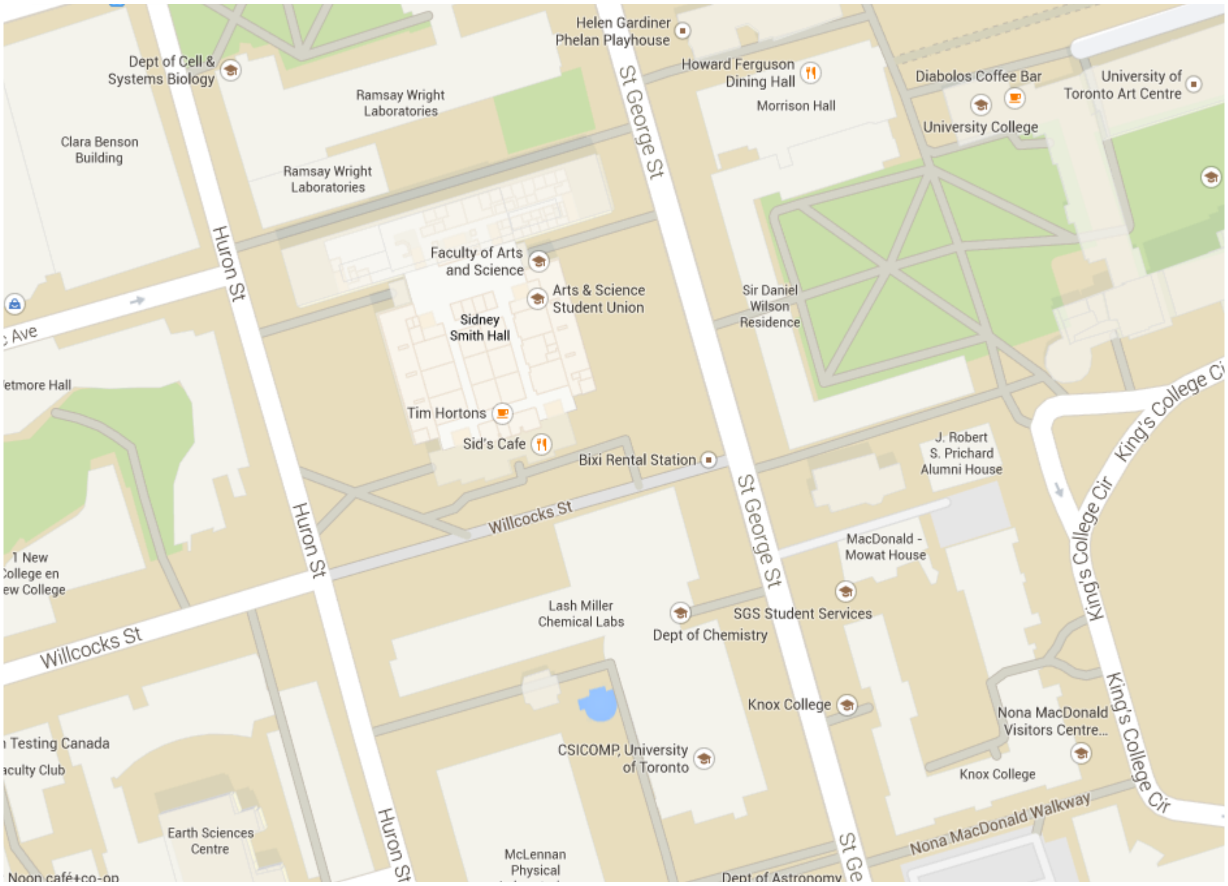

Figure S1: Sampling location (Lash Miller Chemical Laboratories) in the downtown Campus of University of Toronto.

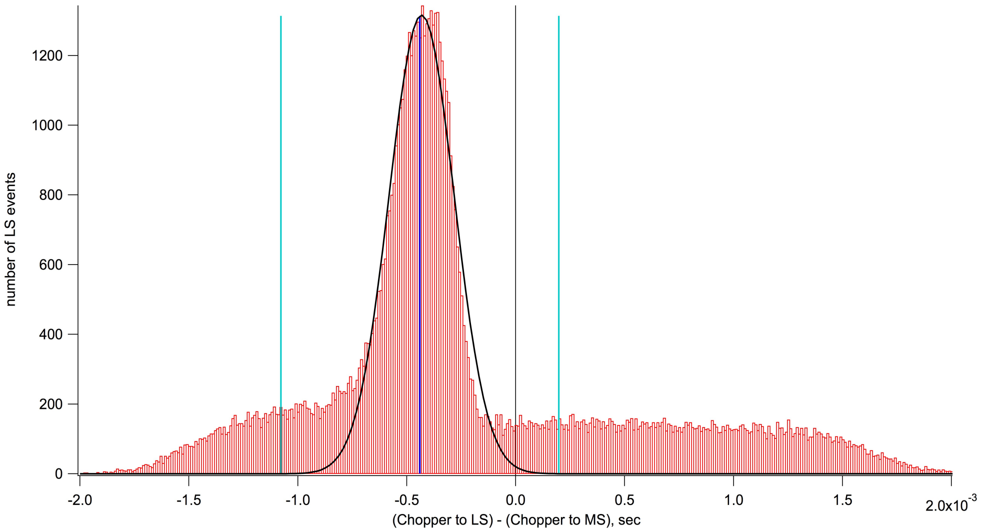

Figure S2: The distribution of the difference between $LS_{PToF}$ and $MS_{PToF}$ (i.e., $LS_{PToF}$ - $MS_{PToF}$) for defining the prompt particle boundaries (i.e., particles falling outside the Gaussian fit boundaries (3σ) were either assigned as "early" or "delayed" particle types).

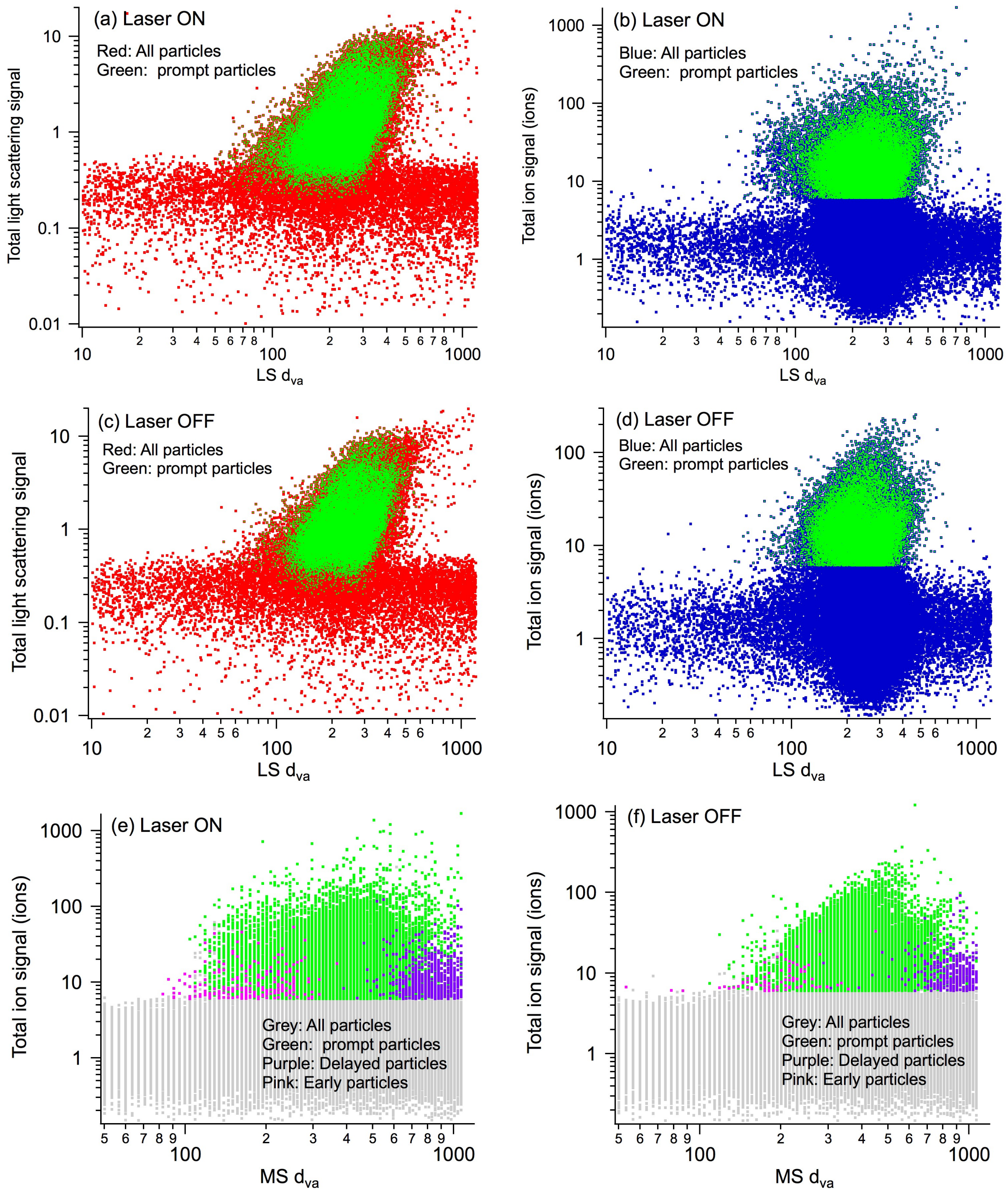

Figure S3: The size distributions (from light scattering signal, LS $d_{va}$) of prompt particles in terms of (a and c) the total light scattering signal intensity and (b and d) the total number of ions in an individual particle. (e and f) The size distributions (from mass spectral signal, MS $d_{va}$) of prompt particles in terms of the total number of ions in an individual particle.

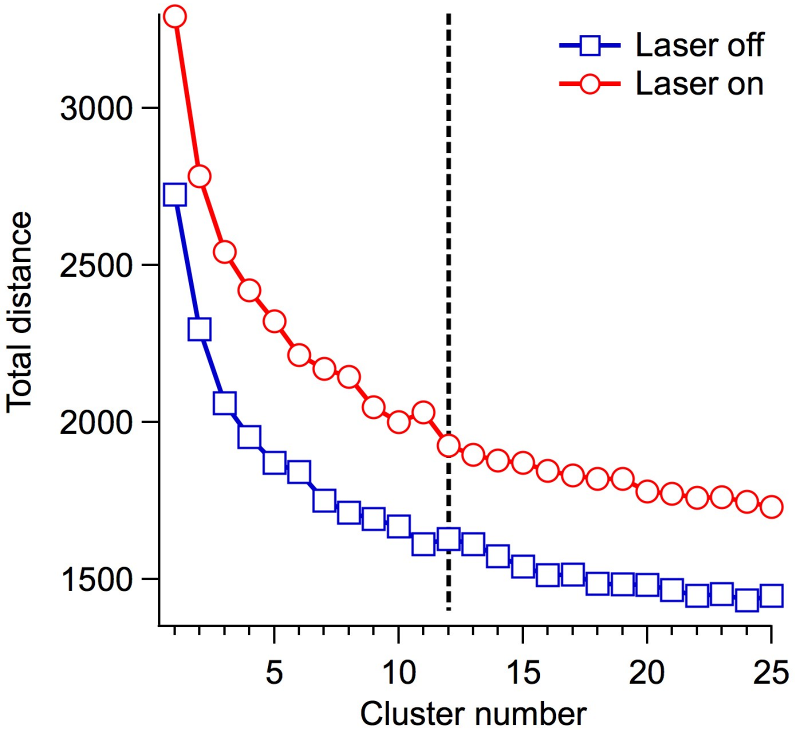

Figure S4: The total distance between the cluster centers and each single particle data obtained from k-means clustering analysis. The dashed line indicates the number of clusters (12) for the interpretation of the mixing state of ambient particles in the current study.

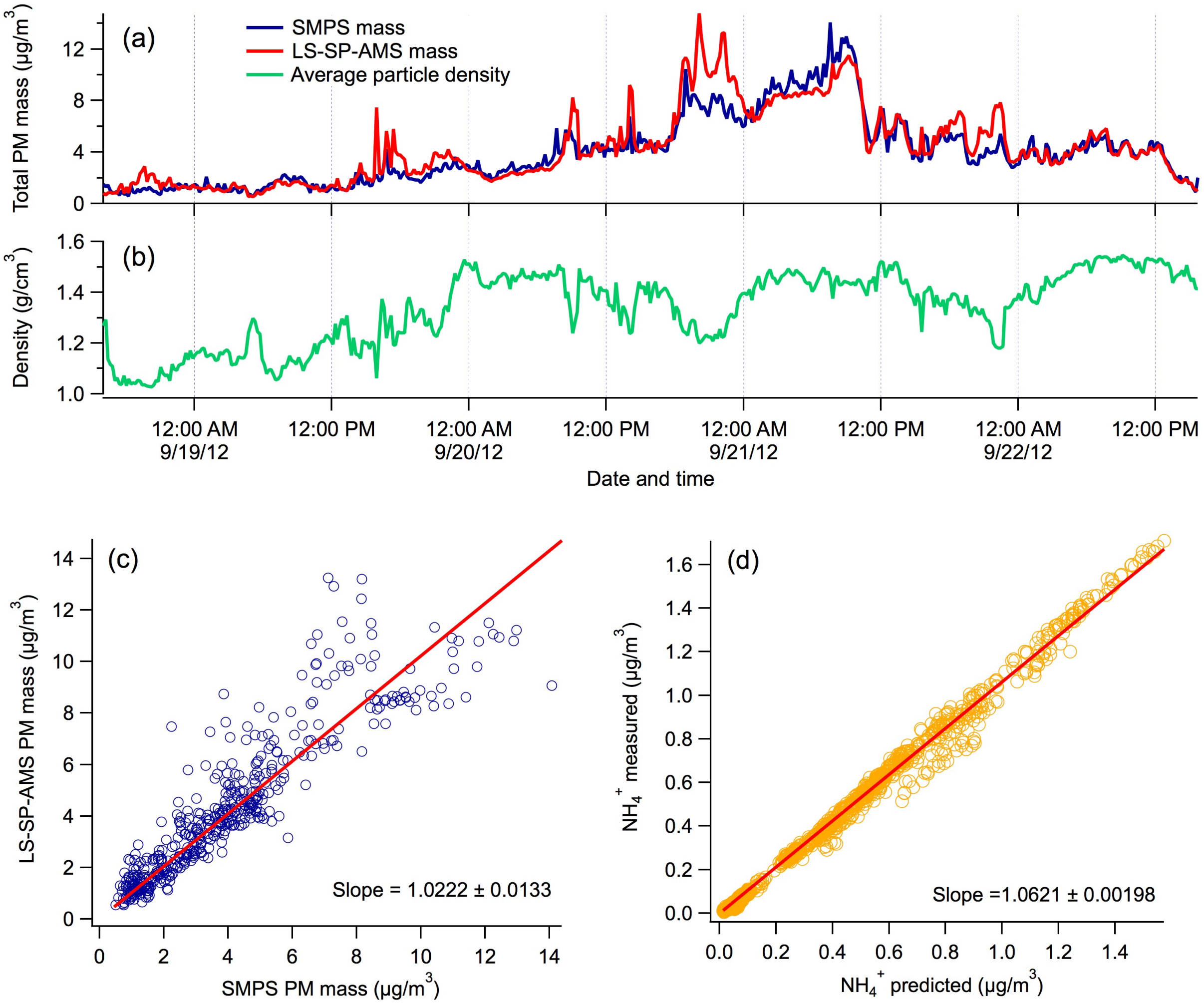

Figure S5: (a) Time series (local time) of particle mass loadings (ammonium + nitrate + sulfate + organics + rBC) determined by LS-SP-AMS laser-off ensemble measurement for NR-PM with CE correction (red) and SMPS measurement (blue). (b) Time series of average particle density determined based on the aerosol composition. Assuming all particles are spherical, the particle volume measured by SMPS can be converted to mass loading using the average particle density (See below for the details of calculation) .(c) Comparison of particle mass loadings measured by LS-SP-AMS and SMPS. (d) Comparison of predicted $NH_4^+$ (assuming complete neutralization of nitrate and sulfate) and measured $NH_4^+$ (directly measured by LS-SP-AMS) mass loading. The slope of a linear fitting is close to 1, suggesting the measured particles are completely neutralized.

### Calculation of PM mass loading from LP-SP-AMS ensemble data:

Due to particle bounce on the tungsten vaporizer, the collection efficiency (CE) of solid/semi-solid particles is approximately equal to 0.5. Typical examples include completely neutralized ambient inorganic sulfate particles (i.e., ammonium sulfate). It is also well know that liquid droplets such as oil droplets and pure ammonium nitrate can stick on the tungsten surface without significant bouncing issue (i.e., CE ~1).

According to our LS-SP-AMS ensemble measurement, sulfate and nitrate were completely neutralized with ammonium as shown in Figure S5d. Although pure ammonium nitrate particles would not undergo crystallization, they were likely internally mixed with sulfate in different extents in accumulation mode particles ($d_{va}$ peak at ~ 400 nm) as discussed in Section 3.5 of the paper. It is reasonable to assume that the CE of all inorganic components (including sulfate, nitrate and ammonium) is equal to 0.5 in this study. In Section 3.2 of the paper, positive matrix factorization identifies three major types of organic aerosols (OA) in this study. They are hydrocarbon-like OA (HOA), Cooking OA (COA) and OOA. HOA and COA are oil-like droplets and are the main contributors to the total organic mass. Hence, CE of total organics is likely close to 1. However, it is worth noting that OOA can be internally mixed with inorganics in accumulation mode as shown in Figure 8 in the manuscript, which may introduce uncertainty to the estimation. The CE of rBC is still highly uncertain. In this calculation, we set the CE of rBC to 1 as discussed in the main text.

### Calculation of average particle density:

The average particle density is calculated using a linear combination of mass fraction of major aerosol particle components measured by the LS-SP-AMS. For inorganic components, the density of ammonium sulfate and ammonium nitrate are 1.77 and 1.72 g/cm$^3$, respectively. The overall density of HOA, COA and OOA are assumed to be 1, 1 and 1.2 g/cm$^3$, respectively. The density of ambient rBC is highly uncertain. As estimation, the effective density of Regal Black, the calibration standard in this study, 0.8 g/cm$^3$, is used. Note that due to a relatively low loading of ambient rBC, the total particle mass loading calculated from SMPS is not sensitive to the effective density of rBC. Besides, the SMPS volume is calculated for spherical particle.

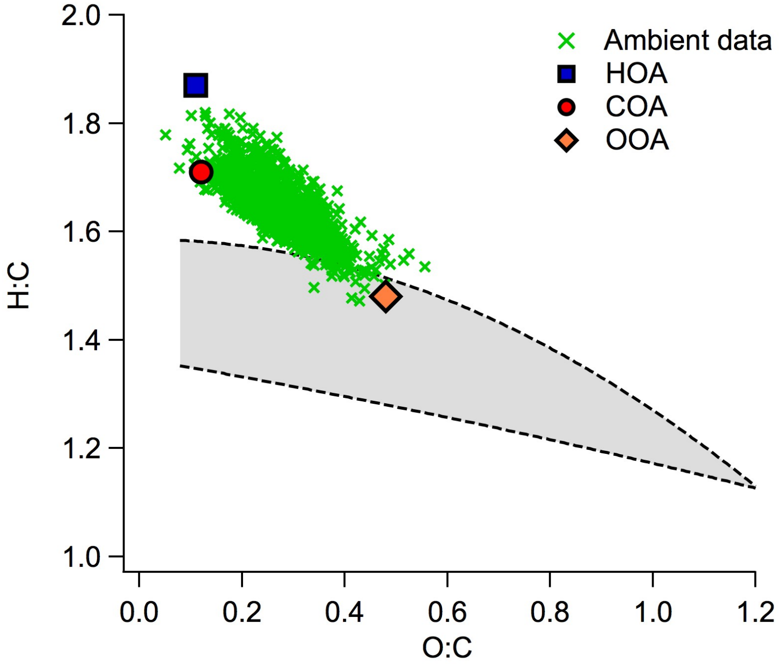

Figure S6: Van-Krevelen diagram: The grey area represents typical values for ambient organic aerosol measured in North Hemisphere (Ng et al. 2010). HOA, COA and OOA coordinates were obtained by PMF analysis of the organic components using the laser-off measurements.

Reference:

Ng, N. L., Canagaratna, M. R., Zhang, Q., Jimenez, J. L., Tian, J., Ulbrich, I. M., Kroll, J. H., Docherty, K. S., Chhabra, P. S., Bahreini, R., Murphy, S. M., Seinfeld, J. H., Hildebrandt, L., Donahue, N. M., DeCarlo, P. F., Lanz, V. A., Prevot, A. S. H., Dinar, E., Rudich, Y. and Worsnop, D. R.: Organic aerosol components observed in Northern Hemispheric datasets from Aerosol Mass Spectrometry, Atmospheric Chemistry and Physics, 10, 4625-4641, 2010.

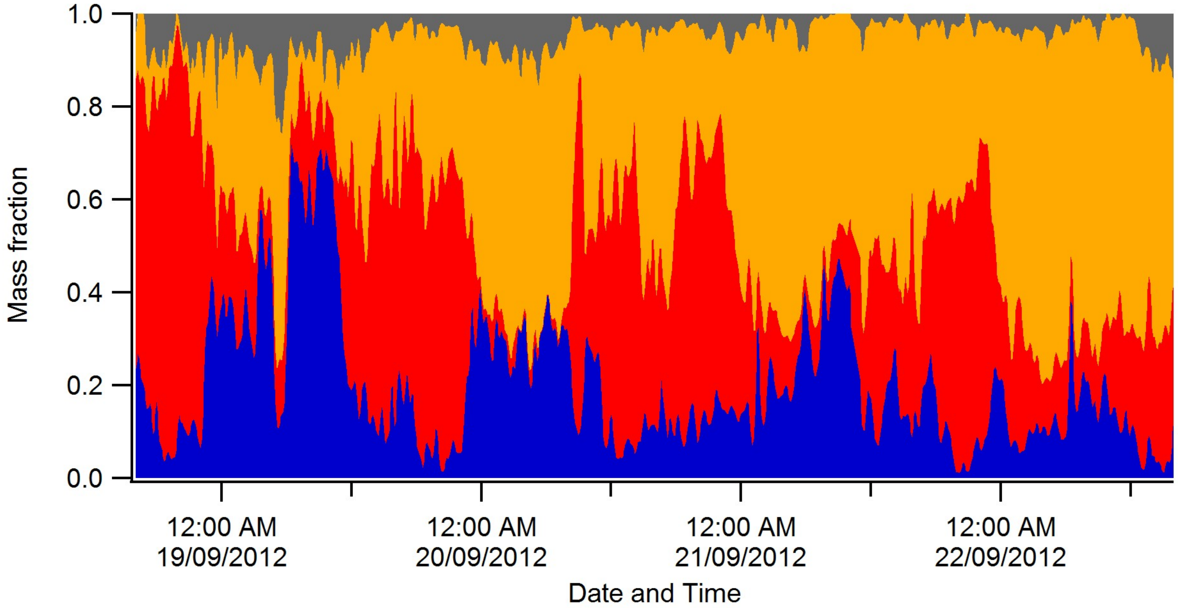

Figure S7: Mass fraction contributions of each PMF factor (Blue: HOA, Red: COA, Orange: OOA, Grey: Residual) to the total organics from IR laser-off measurement. The relatively high residual for the first two days of our sampling period is mainly due to a low loading of organic aerosol.

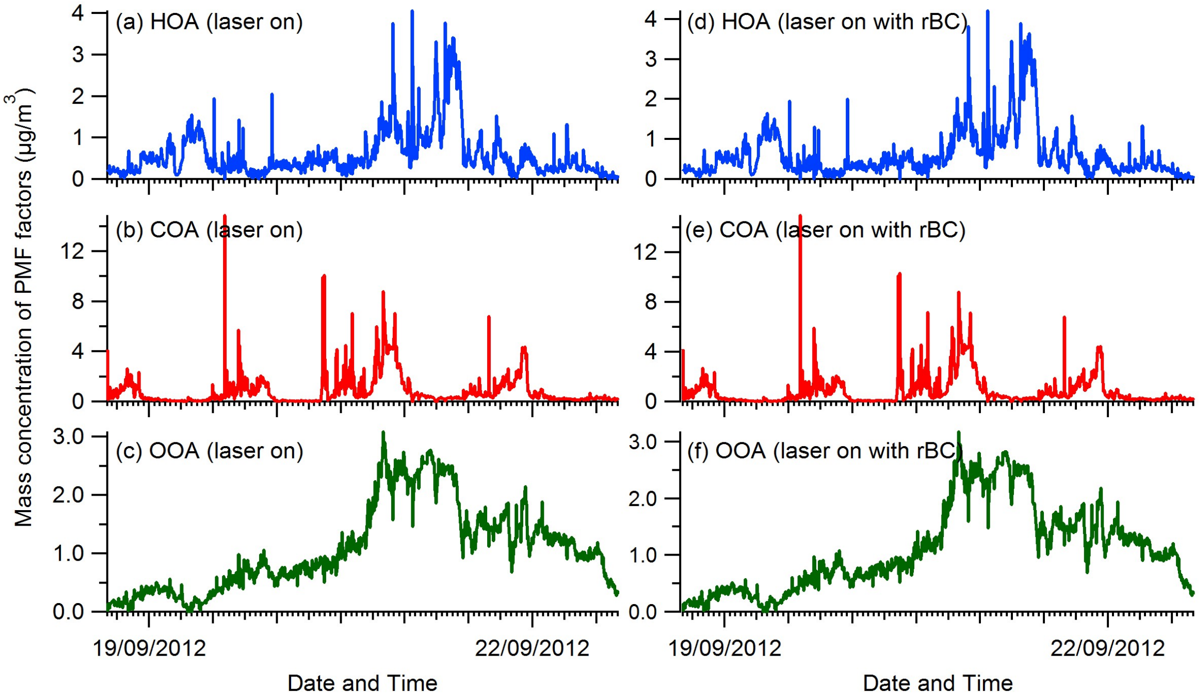

Figure S8: The time series of organic factors obtained from the IR laser-on measurements without (a-c) and including rBC signals (d-f) in the PMF analysis.

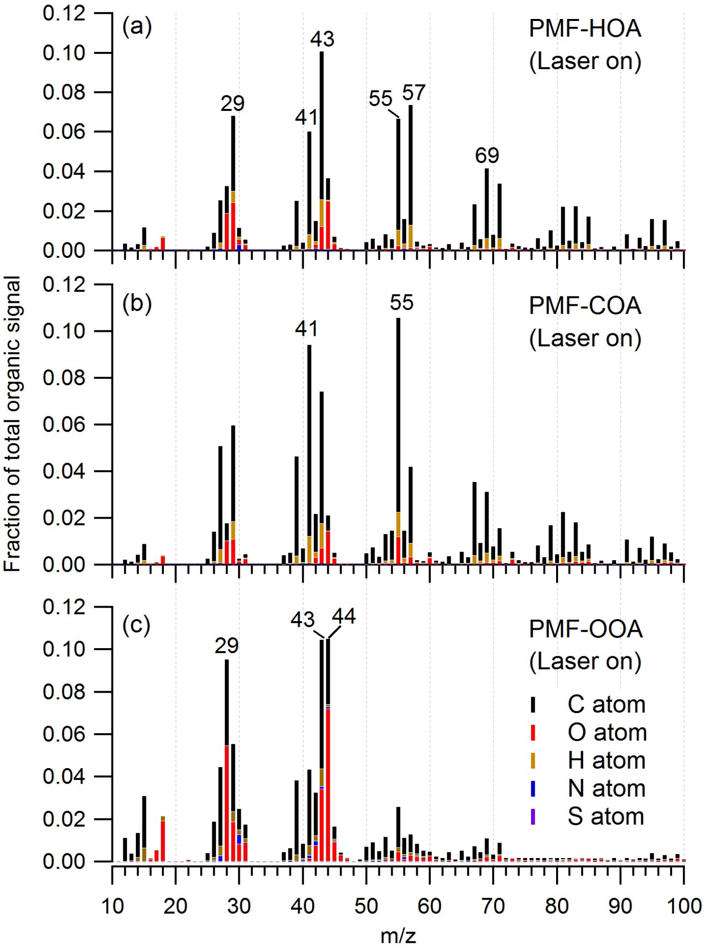

Figure S9: Normalized mass spectra of PMF organic factors from laser-on mode measurement (without rBC signals in the PMF analysis): (a) HOA factor, (b) COA factor, (c) OOA factor.

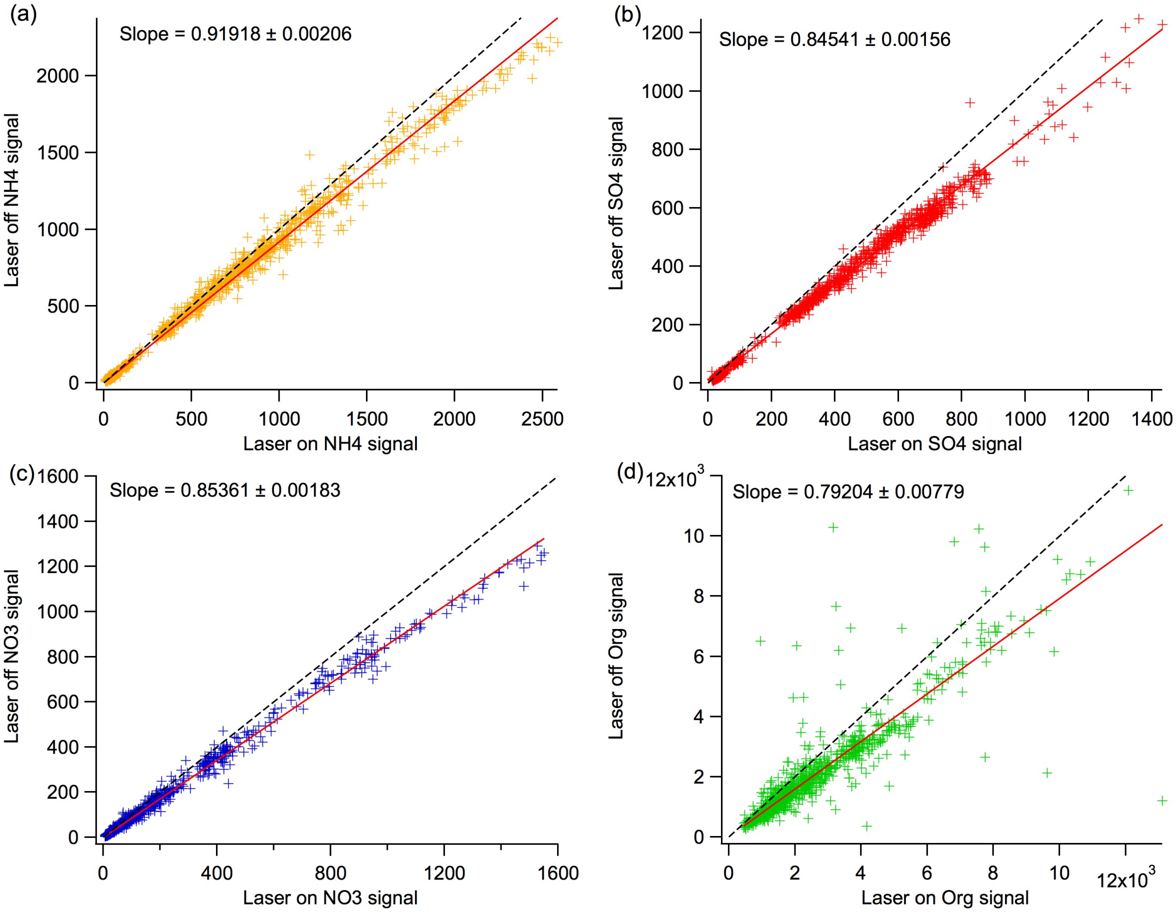

Figure S10: Comparison between the IR laser-on and off measurements (ion signals): (a) $NH_4^+$ (b) $SO_4^{2-}$ (c) $NO_3^-$ and (d) Organic. Dashed line = 1:1 line, red line = data fitting.

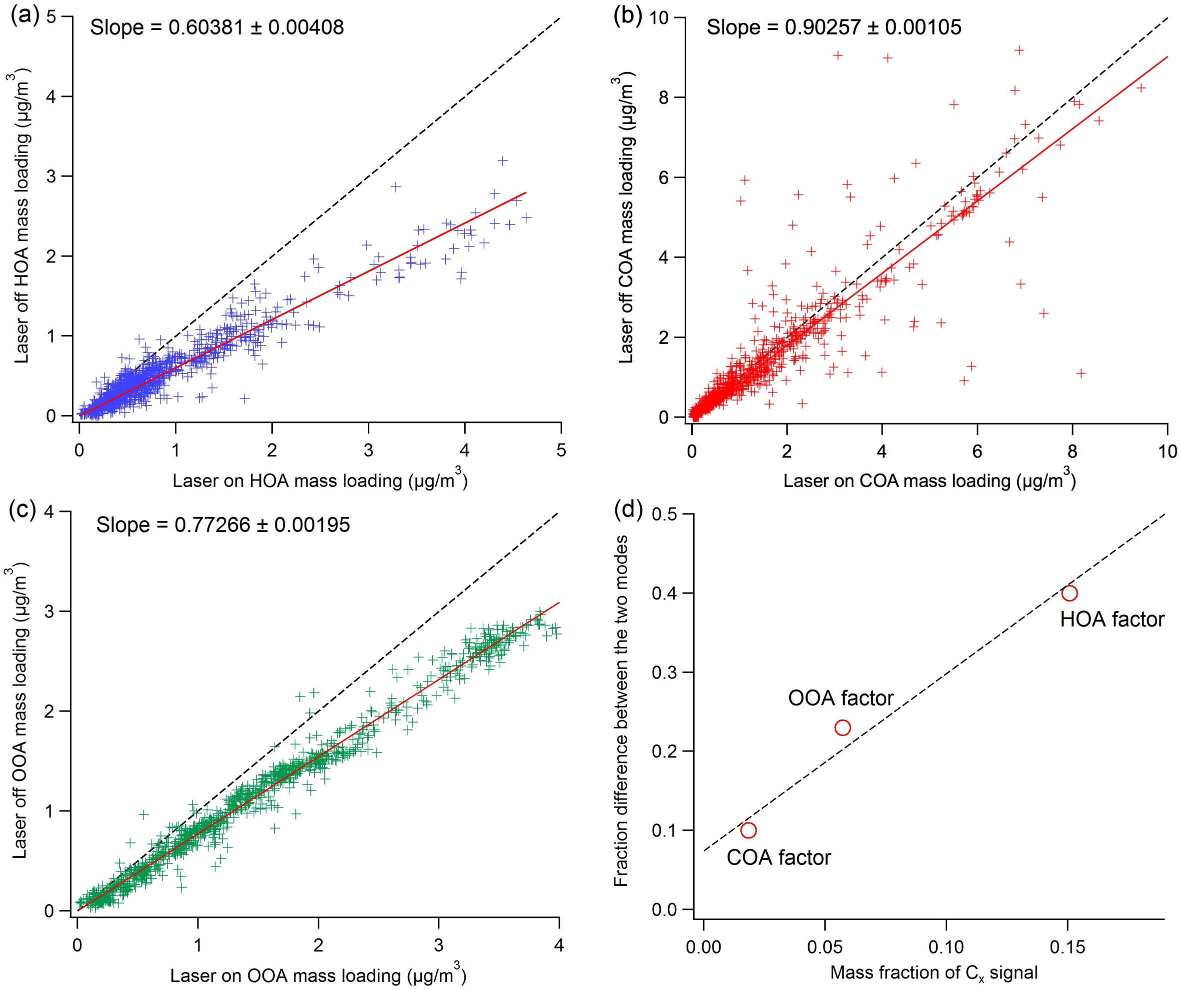

Figure S11: Comparison between PMF results from the IR laser-on and off measurements: (a) HOA (b) COA and (c) OOA. Dashed line = 1:1 line, red line = data fitting. (d) Difference between the two operation modes as a function of rBC fraction. Dashed line = data fitting.

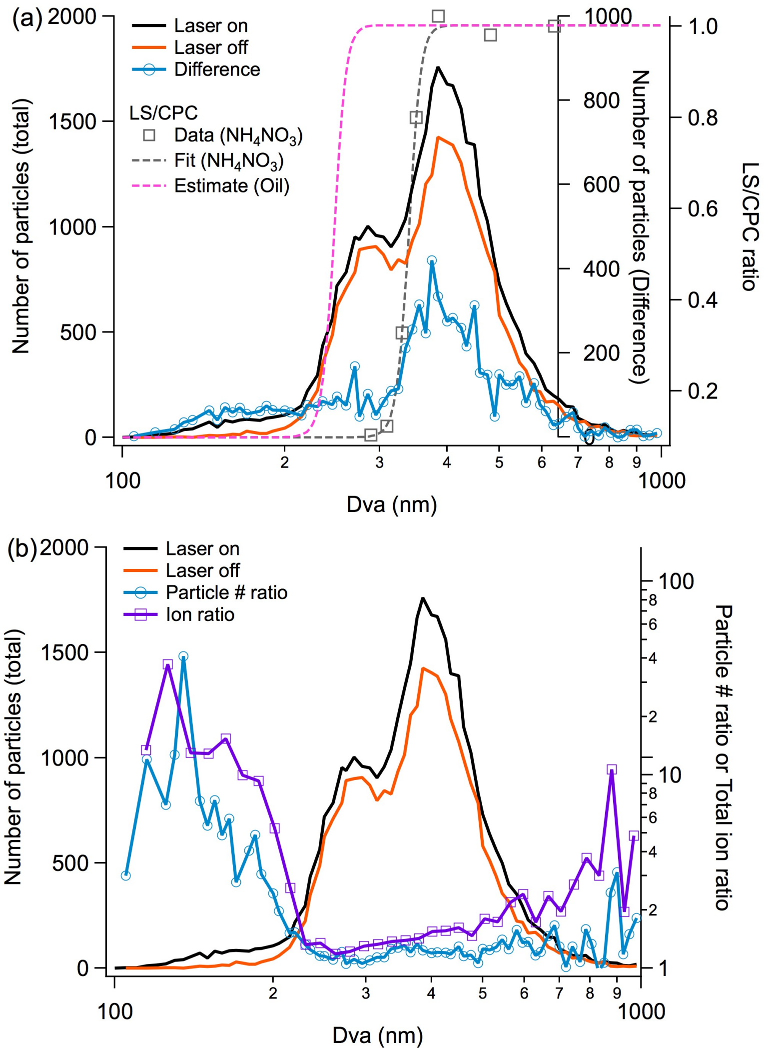

Figure S12: (a) Size distributions of particle number from the ambient single particle measurements (Black: laser-on mode, Orange: laser-off mode, Blue: difference between laser-on and laser-off modes). The grey square (data) and grey dashed line (fitting) represents the counting efficiency (the ratio of light scattering counts and condensation particle counter signals (LS/CPC), left axis) of the light scattering module for ammonium nitrate particles. The pink dashed line indicates an estimated light scattering cut-off $d_{va}$ for spherical hydrocarbon oil droplets (i.e., shape factor = 1 and density = 1 g/cm$^3$). (b) Ratio of particle numbers (Blue circle) and total ion signals (Purple square) between the laser-on and laser-off modes.

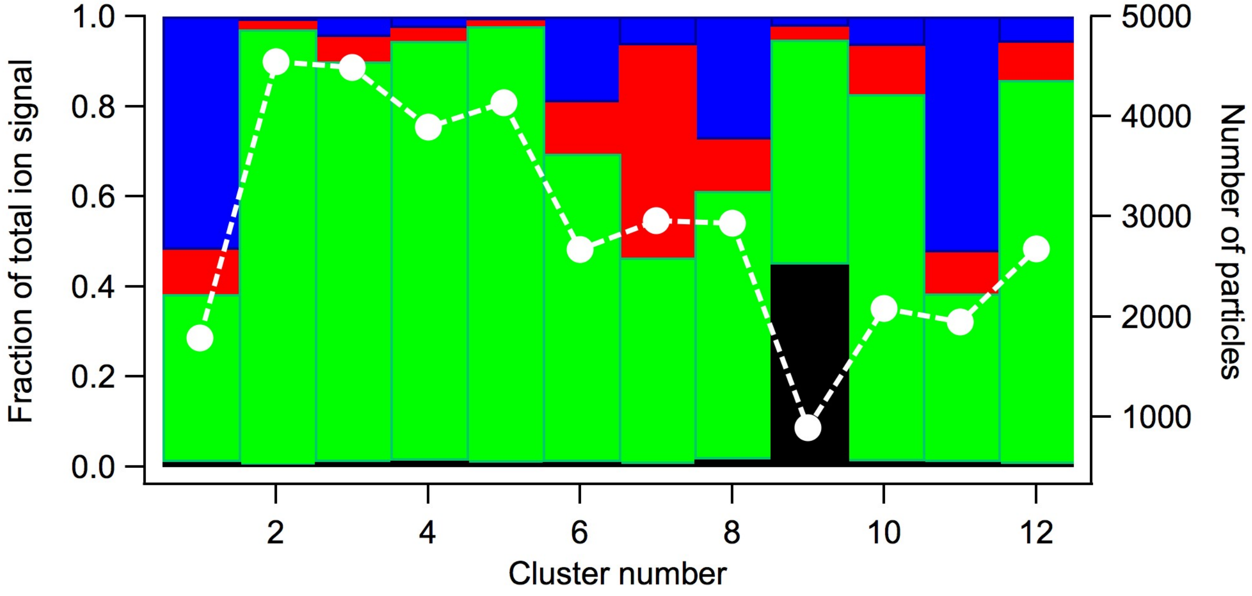

Figure S13: The number of particles (white circles) and the ion fractions of nitrate (blue), sulfate (red), organics (green) and rBC (black) in the 12 preliminary clusters obtained from the k-means clustering analysis.

Nitrate class (Figure 8a) = Clusters 1, 6, 8, and 11

Sulfate class (Figure 8b) = Cluster 7

HOA class (Figure 8c) = Cluster 5

rBC class (Figure 8d) = Cluster 9

COA class (Figure 8e) = Clusters 2 and 4

OOA class1 (Figure 8f) = Cluster 3 and 12

OOA class 2 (Figure 8g) = Cluster 10

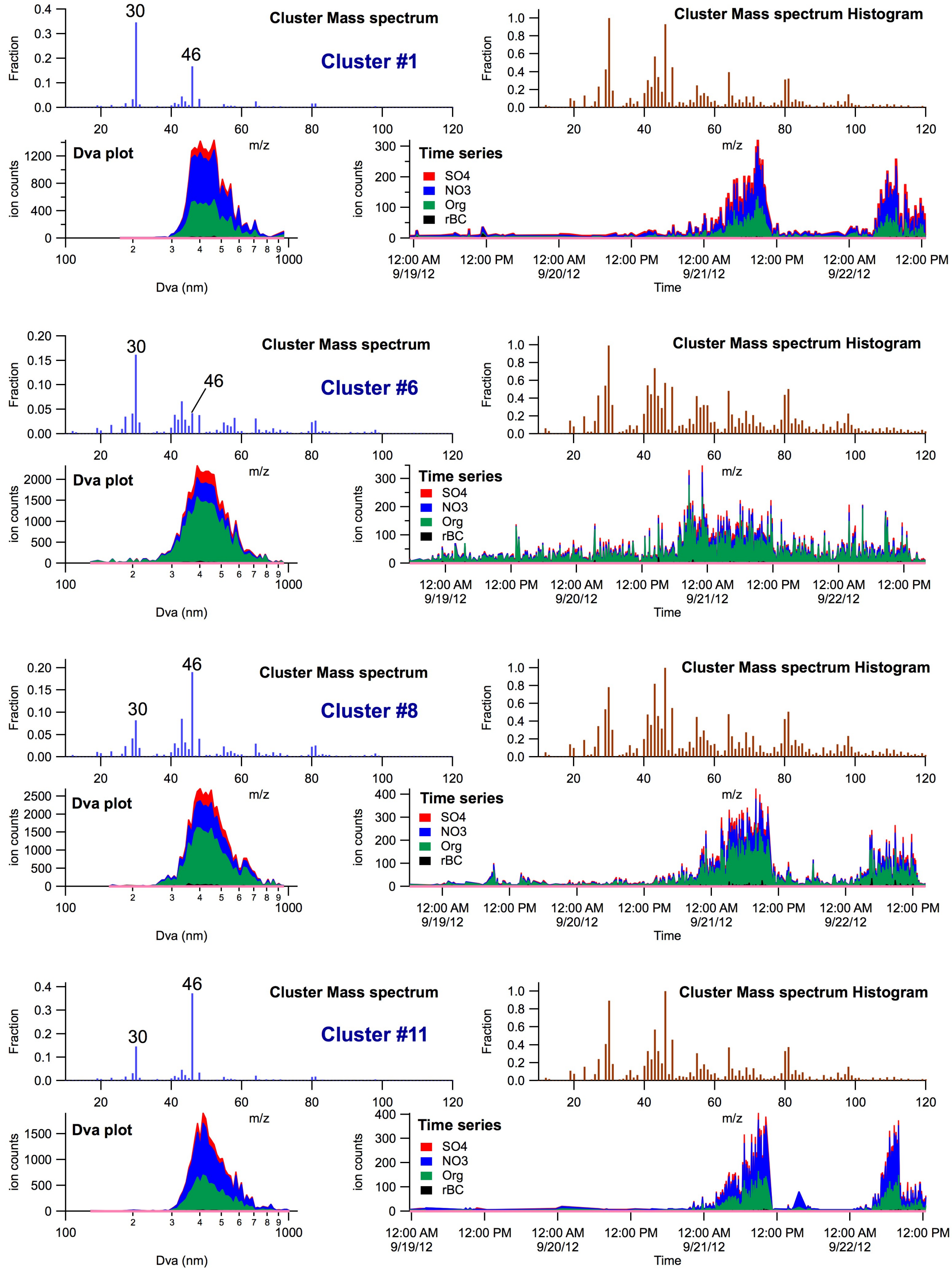

Figure S14: Four preliminary nitrate-rich clusters are combined into a nitrate-rich final particle class, i.e., shown in Figure 8a, h, and p.

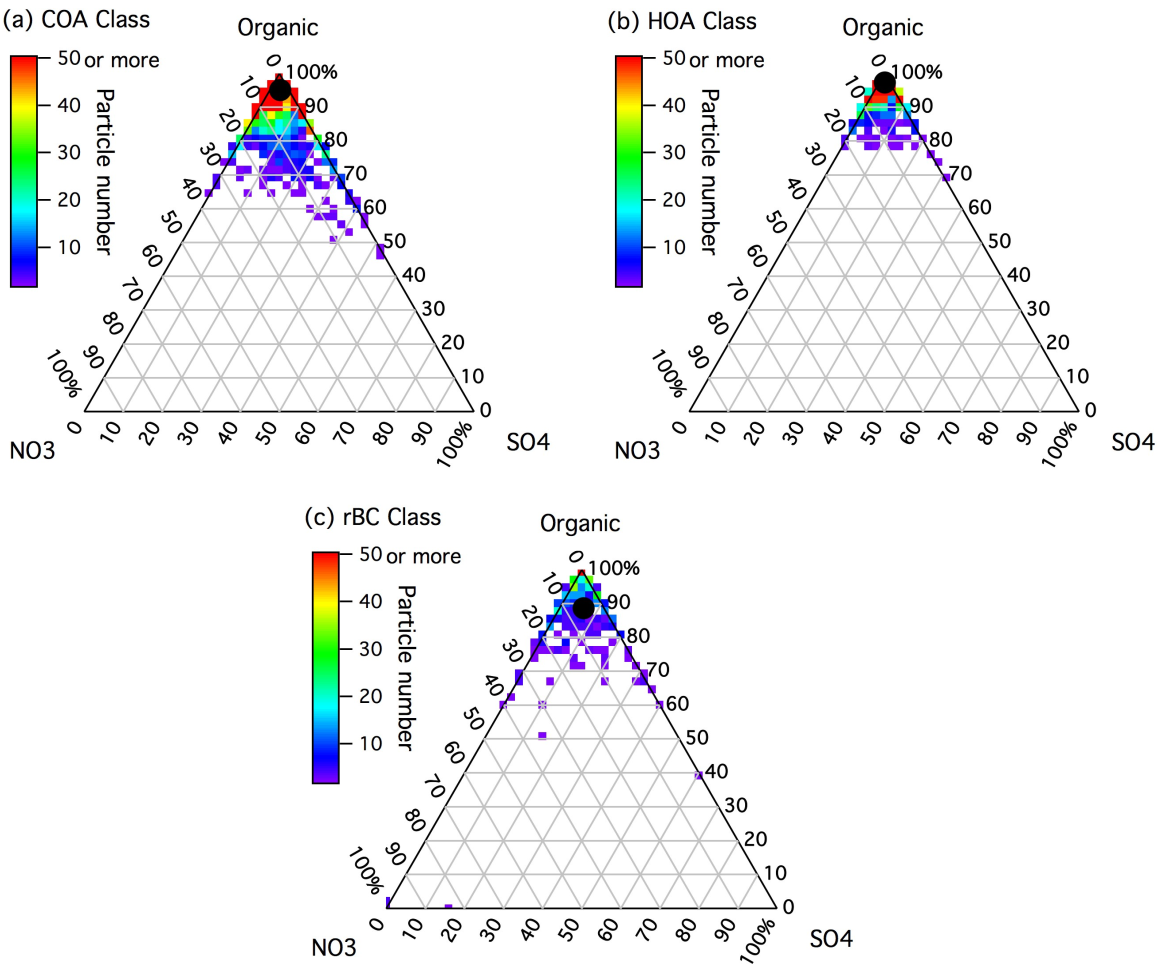

Figure S15: Ternary plot of nitrate, sulfate and organics mass fraction for those particles types identified by cluster analysis of laser-on single particle data: (a) COA, (b) HOA, and (c) rBC. All these particle classes have a relatively low degree of mixing with nitrate and sulfate. The black solid circles indicate the coordinates of average compositions of each particle classes.

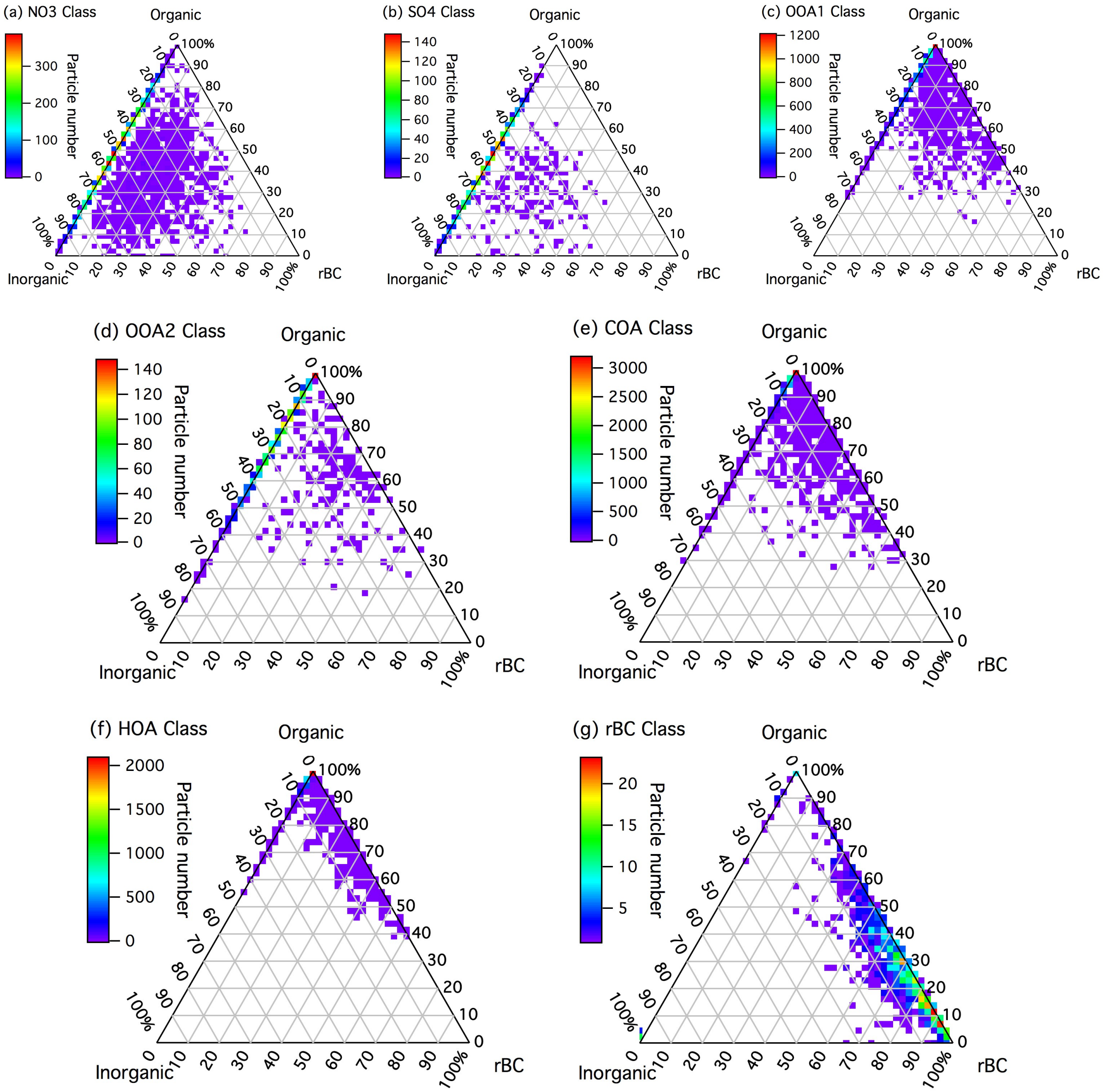

Figure S16: Ternary plot of inorganic, organics and rBC mass fraction for those particles types identified by cluster analysis of laser-on single particle data: (a) Nitrate, (b) Sulfate, (c) OOA1, (d) OOA2, (e) COA, (f) HOA, and (g) rBC.

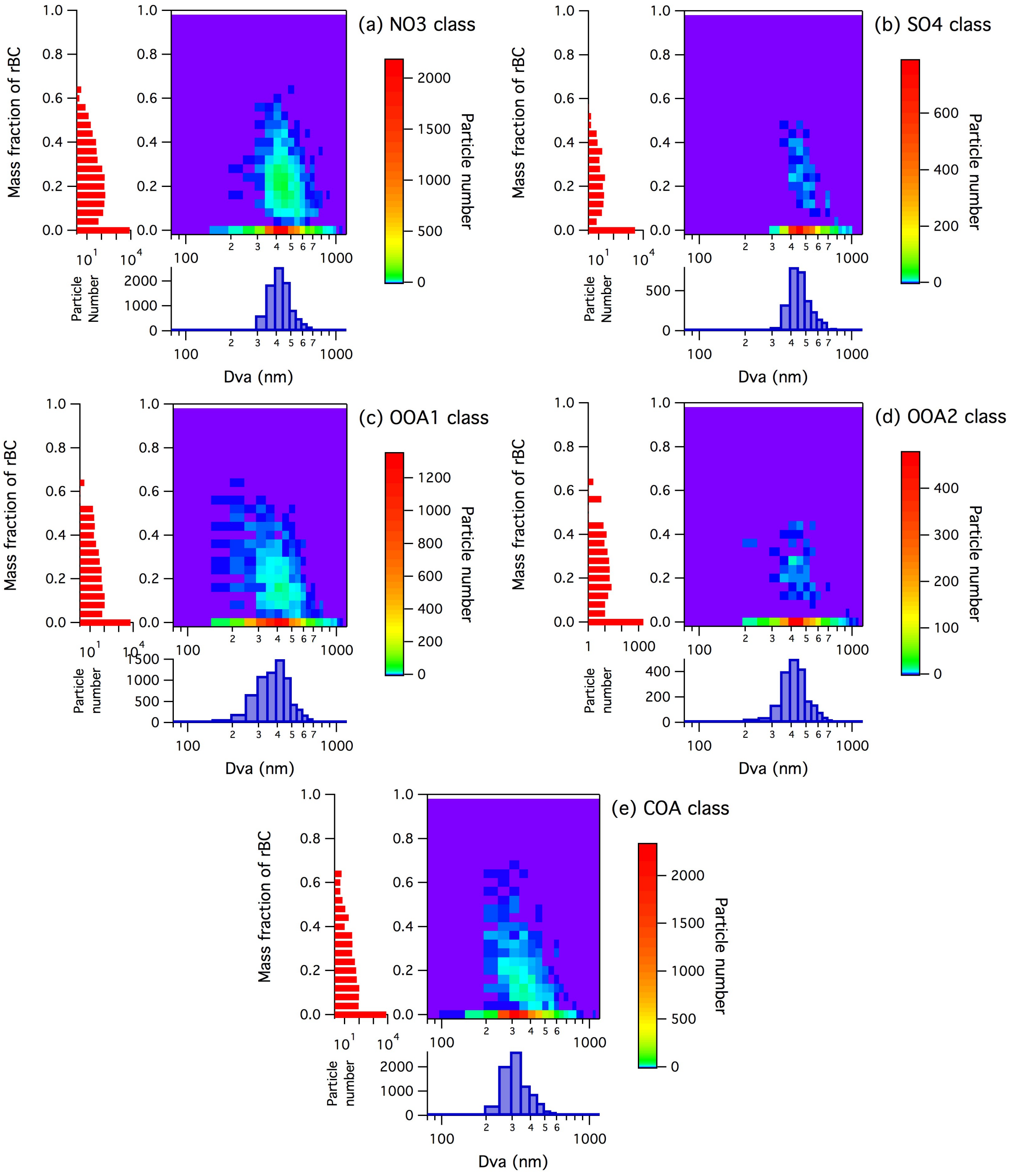

Figure S17: Distributions of particle size and rBC mass fraction of (a) NO3 class, (b) SO4 class, (c) OOA1 class, (d) OOA2 class, and (e) COA class identified by cluster analysis of laser-on single particle data.